ELSEVIER

Polymer 41 (2000) 8673–8679

polymer

www.elsevier.nl/locate/polymer

Formation of polypropylene particles via thermally induced phase separation

H. Matsuyama[a,*], M. Teramoto[a], M. Kuwana[b], Y. Kitamura[b]

[a]*Department of Chemistry and Materials Technology, Kyoto Institute of Technology, Matsugasaki, Sakyo-ku, Kyoto 606-8585, Japan*
[b]*Department of Environmental Chemistry and Materials, Okayama University, 2-1-1 Tsushima-naka, Okayama 700-8530, Japan*

Received 9 February 2000; received in revised form 24 March 2000; accepted 31 March 2000

Abstract

Polypropylene particles were prepared by a thermally induced phase separation. The particle formation occurred by the nucleation and growth mechanism in the metastable region. The particle growth was followed by the dynamic light scattering measurement. Although the growth rates depended on the experimental conditions such as the polymer concentration and temperature, the particle diameter d increased with time t in accordance with the relation of $d^3 \propto t$ in all cases. Detailed consideration on the slope values indicated that the particles grew by the coalescence mechanism. The particle size distribution, which was obtained by SEM observation, became broader when the polymer concentration was higher. © 2000 Elsevier Science Ltd. All rights reserved.

Keywords: Thermally induced phase separation; Polymer particle; Polypropylene

1. Introduction

Polymer particles are of interest as stationary phases in chromatography, adsorbents, catalyst supports and drug delivery system. Techniques for preparing polymer particles are classified into two processes: methods based on polymerization and physico-chemical treatments of polymer solution. The former technique involves emulsion polymerization, seeded emulsion polymerization, emulsifier-free polymerization, suspension polymerization and non-aqueous phase dispersion polymerization. Although these methods have been widely used for preparing polymer particles, the time required for the preparation may be long. Another disadvantage is that they require a lot of chemical substances such as monomer, initiator, emulsifier and so on.

On the other hand, physicochemical treatments of polymer solution such as rapid drying, quenching for phase separation (thermally induced phase separation) and adding precipitants are alternative ways to prepare polymer particles. These methods are generally fast procedures. The concept of particle formation via thermally induced phase separation (TIPS) is shown in Fig. 1. The phase diagram shown in this figure is typical for a crystalline polymer and contains the binodal line showing the border of liquid–liquid phase separation, spinodal line and the crystallization temperature. In the TIPS process, a polymer is dissolved in a diluent at high temperature. Upon removal of the thermal energy by cooling the solution, phase separation is induced when the condition of solution crosses the binodal. When the polymer concentration is lower than that at the critical point, a polymer-rich phase becomes a dispersed phase after the phase separation, while a polymer-lean phase becomes a matrix phase. Thus, the particle formation occurred. On the other hand, when the polymer concentration is higher than that at the critical point, polymer-rich phase becomes the matrix phase, which leads to the porous membrane [1].

Compared with numerous works on the membrane preparation by the TIPS process, there have been reported a few studies on the particle formation. Schaaf et al. prepared polymer particles from crystallization of semi-dilute solutions of polyethylene in poor solvents by the TIPS process [2]. The morphologies reflected the interplay of a liquid–liquid phase separation process and nucleation of the polymer crystals. Liquid–liquid phase separation phenomena that take place prior to crystallization could induce characteristic polymer morphologies. Hou and Lloyd reported the preparation of fairly uniform particles of nylon polymer [3]. The phase separation was done by taking a 1 wt% solution in a theta solvent above the theta temperature and cooling it rapidly. The surface roughness of the particles was dependent on the kind of nylons.

* Corresponding author. Fax: + 81-75-724-7542.
E-mail address: matuyama@chem.kit.ac.jp (H. Matsuyama).

0032-3861/00/$ - see front matter
PII: S0032-3861(00)00268-8

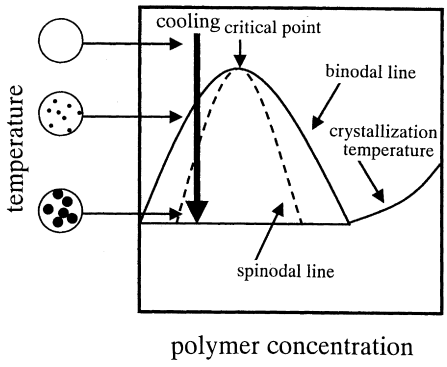

Fig. 1. Particle formation via thermally induced phase separation.

In this work, polypropylene particles were prepared by the TIPS process. The growth of the particle size was measured by a dynamic light scattering method and the particle growth mechanism was discussed.

2. Experimental

2.1. Materials

The polymer used was isotactic polypropylene (iPP, Aldrich Chemical Co., $M_w = 250\,000$). Diphenyl ether (DPE, Nacalai Tesque Co., Japan) and methyl salicylate (MS, Nacalai Tesque Co., Japan) were used as diluent without further purification.

2.2. Measurement of particle size

A glass bottle including weighed polymer and diluent was heated at 433 K for 30 min to make homogeneous polymer solution. Then, the solution was quickly poured and cooled in a cell for a dynamic light scattering (DLS) measurement. The diameter of the particle formed by the phase separation was measured by the DLS apparatus (Otsuka Electronics, Co., DLS-7000). The measurement angle was 90° and the accumulation was done 10 times. Cumulant method was used as the data analysis method. The cell temperature in the DLS apparatus was controlled at the desired constant value. Fig. 2 shows the temperature changes of the solutions

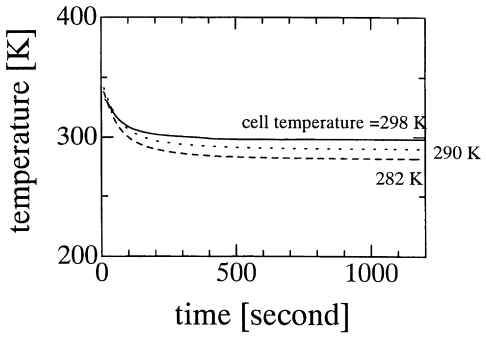

Fig. 2. Temperature changes of solutions in the DLS measurement cell. iPP–MS system, polymer concentration = 0.01 wt%.

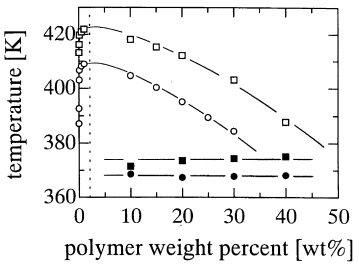

Fig. 3. Phase diagram of two polymer–diluent systems. □: cloud point curve in iPP–MS system, ○: cloud point curve in iPP–DPE system, ■: crystallization temperature in iPP–MS system, ●: crystallization temperature in iPP–DPE system.

in the DLS measurement cell controlled at several temperatures. When the hot homogeneous solution was poured in the cell, temperature approached the constant value after about 5 min. Therefore, data of the particle diameter after 5 min were adopted.

2.3. Phase diagram

Cloud point curves were determined as follows. For polymer samples at the concentration higher than the critical point, homogeneous solid polymer–diluent samples were prepared by a method previously described [4]. Each solid sample was chopped into small pieces and placed between a pair of microscope cover slips. To prevent diluent loss by evaporation, a Teflon film of 100 μm thickness with a square opening in the center was inserted between the cover slips. In the case of the polymer concentration below the critical point, the homogeneous solutions were prepared by heating the glass bottle including iPP and diluent at 433 K for 30 min. Then the homogeneous solution was sandwiched between two cover slips. Each cover slip sample was heated on a hot stage (Linkam, LK-600PH) at 433 K for 5 min and then cooled at a controlled rate of 10 K/min. Cloud points were determined visually by noting the appearance of turbidity under the microscope.

A DSC (Perkin Elmer DSC-7) was used to determine the crystallization temperature for the dynamic phase diagram. A solid polymer–diluent sample was sealed in an aluminun DSC pan, melted at 473 K for 5 min and then cooled at a controlled rate of 10 K/min to 298 K. The onset of the exothermic peak during the cooling was taken as the crystallization temperature.

2.4. SEM observation

The homogeneous polymer solution heated at 433 K was poured and cooled in the DLS measurement cell. The cell was set in the DLS apparatus and held for 1 h at 298 K for the growth of the particle. Then, the solution including the polymer particles was poured in an aluminun pan and the diluent was evaporated for about 1 day. The dried polymer particles were sputtered with Au/Pd in vacuum and

Table 1
Molar volumes and fractions of critical point

System	v_1 (cm^3/mol)	v_2 (cm^3/mol)[a]	$\phi_{2,c}$	$w_{2,c}$
iPP–DPE	164	278 000	0.024	0.021
iPP–MS	137	278 000	0.022	0.018

[a] This value was taken from M_w.

observed by SEM (Hitachi co., S-2150) under an accelerating voltage of 15 kV.

3. Results and discussion

3.1. Phase diagram

Fig. 3 shows the phase diagram of two polymer–diluent systems. iPP–MS system showed the higher cloud point curve. The solubility parameters for iPP, DPE and MS were reported as 18.8 MPa$^{1/2}$ [5], 20.7 MPa$^{1/2}$ [6] and 21.7 MPa$^{1/2}$ [5], respectively. The difference in the solubility parameters between iPP and MS is larger than that between iPP and DPE, which means that iPP–MS system is less compatible. The less compatibility leads to the higher cloud point temperature, as shown in Fig. 3. As a first approximation, the cloud points were assumed to be representative of the coexistence curve [7]. The crystallization temperature was not influenced so much by the kind of diluents.

According to Flory–Huggins theory [8], a polymer volume fraction at the critical point $\phi_{2,c}$ can be obtained by Eq. (1):

$$\phi_{2,c} = \frac{1}{1 + (v_2/v_1)^{1/2}} \tag{1}$$

Here, v_1 and v_2 denote the molar volume of diluent and polymer, respectively. $\phi_{2,c}$ and a polymer weight fraction at the critical point $w_{2,c}$, which was estimated from $\phi_{2,c}$, are summarized in Table 1 along with values of v_1 and v_2. Since values of $w_{2,c}$ in two systems are almost the same, $w_{2,c}$ in iPP–MS system is shown as vertical dotted line in Fig. 3. The values of $w_{2,c}$ are about 2 wt%, which indicates that polymer particle can be obtained when the polymer concentration is less than about 2 wt% in the case of shallow quench. If the concentration is higher than 2 wt%, porous membranes will be formed.

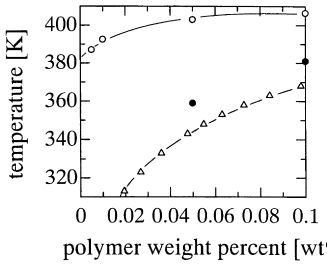

Fig. 4. Enlarged phase diagram in the low polymer concentration region for iPP–DPE system. ○: cloud point curve, △: calculated spinodal temperature, ●: temperature at which turbidity appeared.

Fig. 4 shows an enlarged phase diagram in the low polymer concentration region for iPP–DPE system. Equating polymer chemical potentials in the two phases based on the Flory–Huggins theory gives following two equations describing the binodal curve [7,8]:

$$\{(\phi_2^\beta)^2 - (\phi_2^\alpha)^2\}\chi = \ln\left(\frac{1-\phi_2^\alpha}{1-\phi_2^\beta}\right) + \left(1 - \frac{1}{r}\right)(\phi_2^\alpha - \phi_2^\beta) \tag{2}$$

$$r\{(1-\phi_2^\beta)^2 - (1-\phi_2^\alpha)^2\}\chi = \ln\left(\frac{\phi_2^\alpha}{\phi_2^\beta}\right) + (r-1)(\phi_2^\alpha - \phi_2^\beta) \tag{3}$$

where ϕ_2^α and ϕ_2^β are the polymer volume fractions in polymer-rich and polymer-lean phases, respectively, χ is the interaction parameter and r the ratio of the polymer molar volume to the diluent molar volume. By using ϕ_2^α shown in Fig. 3 and Eqs. (2) and (3), χ at each temperature was estimated. The interaction parameter was found to have a temperature dependence of $\chi = -1.46 + 813/T$. Spinodal point is obtained from Eq. (4) [9]:

$$\frac{1}{v_1(1-\phi_2)} + \frac{1}{v_2\phi_2} - \frac{2\chi}{v_1} = 0 \tag{4}$$

The spinodal points calculated by using estimated interaction parameter χ are plotted in Fig. 4 as Δ. The region between the binodal and spinodal is a metastable region. Phase separation takes place by the nucleation and growth (NG) mechanism in this region. On the other hand, the spinodal decomposition (SD) occurs in an unstable region enclosed by the spinodal line. When the hot homogeneous polymer solution was cooled in the DLS measurement cell controlled at 298 K, the temperatures at which turbidity appeared, that is, phase separation occurred, were measured and are plotted in Fig. 4 and shown with ●. Those points are in the metastable region and thus, the phase separation mechanism in this work is the nucleation and growth mechanism. When the polymer-rich and polymer-lean phases, which are formed by NG mechanism, are further cooled to 298 K, there is a possibility that second phase separation occurs in respective two phases. If it is the case, many small domains are formed in the initial large particles. However, as shown below in SEM photographs of particles, such a double structure was not observed. This is probably because the particle structure was fixed by the crystallization and the second phase separation could not occur.

3.2. Diameter of critical nuclei

In the mestable region, droplets of the polymer-rich phase are formed by the NG mechanism. When a nucleus formed

Table 2
Diameters of critical nuclei (iPP–DPE system)

Polymer concentration (wt%)	Temperature (K)	Diameter of critical nuclei (μm)
0.05	398	4.6
0.05	393	2.5
0.05	388	2.4
0.01	388	24
0.1	388	1.1

at a given instant has a diameter larger than that of a critical nucleus d_c, the nucleus will continue to grow spontaneously. The values of d_c can be estimated theoretically as follows. For the free energy of formation of a nucleus with radius r, $\Delta G(r)$ is given by Eq. (5) [10–12]:

$$\Delta G(r) = (4/3)\pi r^3[\Delta G'_M(\phi_2) - \Delta G_M(\phi_2)] + 4\pi r^2\sigma \quad (5)$$

Here, $\Delta G'_M$ is the average Gibbs' free energy of mixing of coexisting phases when the solution is phase-separated into the polymer-rich and the polymer-lean phases, and ΔG_M the Gibbs' free energy of mixing per unit volume when the solution is homogeneous. ϕ_2 denotes the polymer volume fraction and σ is the interfacial tension between the nucleus and matrix phase. According to Flory–Huggion theory, ΔG_M is expressed as [8]:

$$\Delta G_M(\phi_2) = RT\{(1 - \phi_2/v_1)\ln(1 - \phi_2) + (\phi_2/v_2)\ln \phi_2 + \chi[(1 - \phi_2)/v_1]\phi_2\} \quad (6)$$

$\Delta G'_M$ is given by the following equation [11]:

$$\Delta G'_M(\phi_2) = [\Delta G_M(\phi_2^\alpha) - \Delta G_M(\phi_2^\beta)](\phi_2 - \phi_2^\beta)/(\phi_2^\alpha - \phi_2^\beta) + \Delta G_M(\phi_2^\beta) \quad (7)$$

Here, superscripts α and β denote the polymer-rich and polymer-lean phases, respectively. $\Delta G(r)$ has a maximum at a radius of the critical nuclei r_c. By applying the condition of $\partial\Delta G(r)/\partial r = 0$ to Eq. (5), the diameter of the critical nucleus is given by

$$d_c = 2r_c = -4\sigma/(\Delta G'_M - \Delta G_M) \quad (8)$$

To estimate d_c, the interfacial tension σ must be known. Heinrich and Wolf measured the interfacial tension between the coexisting phases of the systems polystyrene/methylcyclohexane and polystyrene/cyclohexane [13]. The following generalized equation useful at least for typical vinyl polymers was presented:

$$\sigma(\text{mN/m}) = 0.153N_u^{0.5}\Delta\phi_2^{3.85} \quad (9)$$

Here N_u is the number of monomeric units, and $\Delta\phi_2$ the difference in the polymer volume fractions in the coexisting phases. The interfacial tension was estimated by Eq. (9) in this work.

The values of d_c calculated by Eq. (8) are summarized in Table 2. At constant polymer concentration, d_c decreases with the decrease of temperature. The increase of the polymer concentration brings about the decrease of d_c at constant temperature. These results indicate that d_c becomes smaller when the solution is deeply quenched in the metastable region. This tendency is in agreement with result by Kamide et al. [11].

3.3. Particle growth followed by DLS

Fig. 5 shows the relations between the average particle diameter and time in iPP–DPE system. Several polymer concentration data are shown in this figure. The diameters were larger when the polymer concentrations were higher. In all cases, the average diameters were approximately proportional to time to the power of 1/3. It is interesting to compare the measured average diameters and the calculated diameter of the critical nucleus. The diameter of the critical nucleus formed in 0.1 wt% polymer concentration and at 388 K are shown as dotted line in Fig. 5. This is one of the data listed in Table 2. The temperature at which the nucleation occurs is 382 K in 0.1 wt% concentration, as shown in Fig. 4 and is somewhat different from the

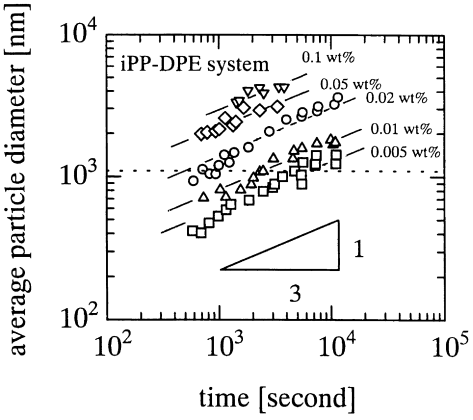

Fig. 5. Relation between average particle diameter and time in iPP–DPE system. Cell temperature = 298 K.

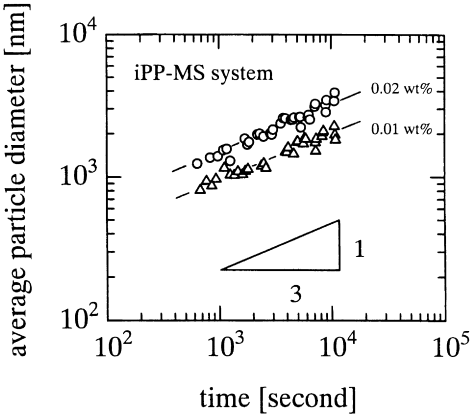

Fig. 6. Relation between average particle diameter and time in iPP–MS system. Cell temperature = 298 K.

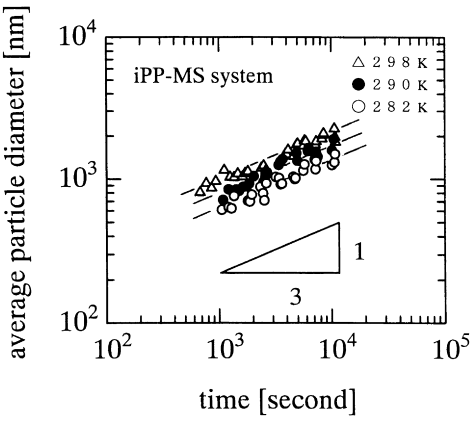

Fig. 7. Effect of temperature on the particle growth. iPP–MS system, polymer concentration = 0.01 wt%.

calculation condition of 388 K. The calculated value of d_c is much lower than the measured initial particle diameters in the 0.1 wt% condition (∇).

Results in iPP–MS system are shown in Fig. 6. The detailed comparison between Figs. 5 and 6 indicates that iPP–MS system had the larger particle size than iPP–DPE system at the same condition. Fig. 7 shows the effect of temperature on the particle growth. The increase of temperature brought about the increase of the particle size. One third dependence on time was also observed in Figs. 6 and 7.

The scaling exponent of 1/3 obtained in this work indicates that the coarsening of droplets obeys the coalescence mechanism or the Ostwald ripening mechanism [14]. In the coalescence mechanism based on the droplet diffusion, the following relation holds between the droplet diameter d and time t when d is much larger than d_c [10]:

$$d^3 = 8kTv/(\pi\mu)t \quad (10)$$

Here, k is the Boltzman constant, v the volume fraction of particles and μ the viscosity of the medium. On the other hand, the Ostwald ripening mechanism gives Eq. (11) according to Lifshitz and Slyozov theory [15,16]:

$$d^3 = (64\sigma D_m c v_m)/(9RT)t \quad (11)$$

Here, D_m is the diffusion coefficient of particle phase substance in the matrix phase, c the molar fraction of the particle phase in the matrix phase, v_m the molar volume of the particle phase and R the gas constant.

As can be seen in Figs. 5–7, the particle diameters were approximately proportional to $t^{1/3}$ for all cases. Thus there are linear relationships between d^3 and t. The experimental data of the slope values in the relation between d^3 and t are summarized in Table 3 along with the calculated slope values by Eqs. (10) and (11). For all cases, the slope values calculated by Eq. (10) are roughly in agreement with the experimental results. However, Eq. (11) gives much smaller values despite

Table 3
Slope values in the relation of d^3 and t

System	Polymer concentration (wt%)	Temperature (K)	Experimental slope value (m^3/s)	Slope value calculated by Eq. (10) (m^3/s)	Slope value calculated by Eq. (11)[a] (m^3/s)	v[b]	μ (Pa s)	σ[c] (N/m)
iPP–DPE	0.005	298	1.76×10^{-22}	3.47×10^{-22}	1.97×10^{-26}	1.28×10^{-4}	3.86×10^{-3}	4.95×10^{-4}
	0.01	298	5.93×10^{-22}	6.91×10^{-22}	3.94×10^{-26}	2.55×10^{-4}	3.86×10^{-3}	4.95×10^{-4}
	0.02	298	1.95×10^{-21}	1.38×10^{-21}	7.88×10^{-26}	5.10×10^{-4}	3.86×10^{-3}	4.95×10^{-4}
	0.05	298	1.00×10^{-20}	3.47×10^{-21}	1.97×10^{-25}	1.28×10^{-3}	3.86×10^{-3}	4.95×10^{-4}
	0.1	298	2.74×10^{-20}	6.91×10^{-21}	3.95×10^{-25}	2.55×10^{-3}	3.86×10^{-3}	4.95×10^{-4}
iPP–MS	0.01	298	8.52×10^{-22}	1.38×10^{-21}	8.15×10^{-26}	2.46×10^{-4}	1.87×10^{-3}	1.02×10^{-3}
	0.02	298	3.14×10^{-21}	2.76×10^{-21}	1.63×10^{-25}	4.92×10^{-4}	1.87×10^{-3}	1.02×10^{-3}
	0.01	290	5.07×10^{-22}	6.97×10^{-22}	8.37×10^{-26}	2.46×10^{-4}	3.60×10^{-3}	1.02×10^{-3}
	0.01	282	2.44×10^{-22}	5.20×10^{-22}	8.63×10^{-26}	2.46×10^{-4}	4.68×10^{-3}	1.02×10^{-3}

[a] In this calculation, polymer diffusion coefficient (1.0×10^{-15} m^2/s [17]) was used as D_m. Molar volume of polymer (0.278 m^3/mol) and initial polymer concentration were used as v_m and c, respectively. The slope values by Eq. (11) was overestimated by this assumption.
[b] Particle volume fraction when the binodal crosses the crystallization temperature.
[c] $\Delta\phi_2$ used in the estimation by Eq. (9) was the value when the binodal crosses the crystallization temperature.

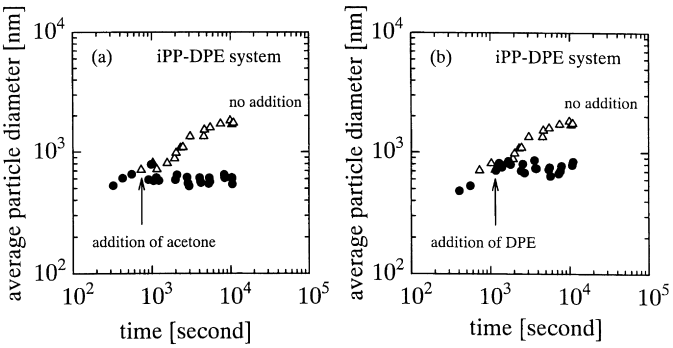

Fig. 8. Effect of addition of diluent on particle growth: (a) addition of acetone; (b) addition of DPE.

the overestimation described in the footnote of Table 3. Thus, it is concluded that particle growth proceeds by the coalescence mechanism rather than by the Ostwald ripening mechanism. The increase of the polymer concentration brings about the increase of v in Eq. (10), which results in the larger particle size, as shown in Figs. 5 and 6. The larger particle size in iPP–MS system than in iPP–DPE is attributable to the lower viscosity μ shown in Table 3. The increase of the particle size brought about by the higher temperature shown in Fig. 7 also attributes to the lower viscosity.

When the particle growth mechanism is coalescence mechanism, the growth rate must be lowered by the addition of a large amount of diluent to the solution because the particle volume fraction v decreases and there are few chances to contact each other. Fig. 8 shows the changes of particle diameters when DPE or acetone was added to the solution. The particle growths were obviously stopped by the addition of DPE or acetone.

3.4. SEM observation of particles

Fig. 9 shows SEM photographs of particles prepared in the different polymer concentration conditions. By measuring the diameters of about 100 particles, the average diameter based on the particle number and standard deviation were obtained. The results are listed in Table 4. The coefficient of deviation CV, which is defined as the standard deviation divided by the average diameter, are also included in this table. As the polymer concentration increased, the average diameter increased, which agrees with the result in Fig. 5. The value of CV also increased with the increase of the polymer concentration. This means that the particle size distribution became broader when the polymer concentration was higher. Generally, occurrence of the coalescence between the particles makes the particle size distribution broader. The broader distribution obtained in the higher polymer concentration is due to the frequent coalescence brought about by the higher particle volume fraction.

The particle sizes obtained by SEM are smaller than those by DLS shown in Fig. 5. The smaller particle size in the SEM observation is probably due to shrinkage of the particle during the evaporation of diluent.

4. Conclusion

Polypropylene particles were prepared by the TIPS process and particle growth was followed by the DLS measurement. The following conclusions were made:

1. The phase separation occurred in the metastable region and the particle formation mechanism was the nucleation growth (NG) mechanism. The diameters of critical nuclei in the NG mechanism were estimated. The diameters became smaller when the solution was deeply quenched in the metastable region.
2. The particles were larger when the polymer concentration

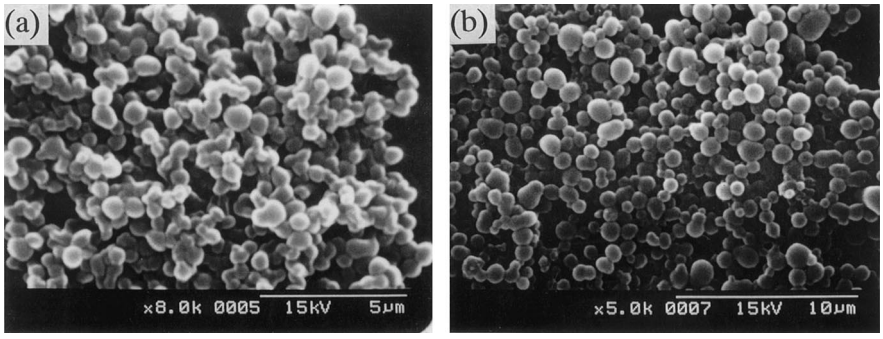

Fig. 9. SEM photographs of particles. iPP–DPE system: (a) polymer concentration = 0.05 wt%, (b) polymer concentration = 0.1 wt%.

Table 4
Size analysis of the particles from SEM (iPP–DPE system)

Polymer concentration (wt%)	Average diameter (μm)	Standard deviation (μm)	Coefficient of deviation
0.05	0.615	0.140	0.228
0.1	0.968	0.254	0.283

was higher or temperature was higher. The particle diameter d increased with time t in accordance with the relation of $d^3 \propto t$ in all cases. From the detailed consideration on the slope values in these relations, it was concluded that the particle grew by the coalescence mechanism.

3. The particles were observed by SEM. The particle size distribution became broader when the polymer concentration was higher.

Acknowledgements

This research was partially supported by HOSOKAWA Powder Technology Foundation.

References

[1] Van de Witte P, Dijkstra PJ, van den Berg JWA, Feijen J. J Membr Sci 1996;117:1.
[2] Scaaf P, Lotz B, Wittmann JC. Polymer 1987;28:193.
[3] Hou W-H, Lloyd TB. J Appl Polym Sci 1992;45:1783.
[4] Kim S-S, Lloyd DR. J Membr Sci 1991;64:13.
[5] Brandrup J, Immergut EH. Polymer handbook. 3rd ed. New York: Wiley, 1989 (chap. 7).
[6] Barton AFM. Handbook of solubility parameters and other cohesion parameters. 2nd ed. Boca Raton: CRC Press, 1991 (chap. 5).
[7] McGuire KS, Laxminarayan A, Lloyd DR. Polymer 1994;35:4404.
[8] Flory PJ. Principles of polymer chemistry. Ithaca: Cornell University Press, 1953 (chap. 13).
[9] Strobl GR. The physics of polymers. 2nd ed. Berlin: Springer, 1996 (chap. 3).
[10] Davies JT, Rideal EK. Interfacial phenomena. 2nd ed. New York: Academic Press, 1963 (chap. 8).
[11] Kamide K, Iijima H, Matsuda S. Polym J 1993;25:1113.
[12] Matsuyama H, Teramoto M, Uesaka T, Goto M, Nakashio F. J Membr Sci 1999;152:227.
[13] Heinrich M, Wolf BA. Polymer 1992;33:1926.
[14] Siggia ED. Phys Rev A 1979;20:595.
[15] Kabalnov AS, Pertzov AV, Shchukin ED. J Colloid Interface Sci 1987;118:590.
[16] Hill MJ, Barham PJ. Polymer 1995;36:3369.
[17] Zeman L, Fraser T. J Membr Sci 1994;87:267.